

Spin-Peierls-like phases in magnetoelastic $J_1 - J_2$ antiferromagnetic chain at $1/3$ magnetization

H.D. Rosales¹ and G.L. Rossini¹

¹*Departamento de Física, Universidad Nacional de La Plata, C.C. 67, 1900 La Plata, Argentina.*

(Dated: February 8, 2022)

We investigate elastic deformations of spin $S = 1/2$ antiferromagnetic $J_1 - J_2$ Heisenberg chains, at $M = 1/3$ magnetization, coupled to phonons in the adiabatic approximation. Using a bosonization approach we predict the existence of non-homogeneous trimerized magnetoelastic phases. A rich ground state phase diagram is found, including classical and quantum plateau states for the magnetic sector as well as inequivalent lattice deformations within each magnetic phase. The analytical results are supported by exact diagonalization of small clusters.

PACS numbers: 75.10.Jm, 73.43.Nq, 75.30.-m

I. INTRODUCTION

Frustrated spin systems have been continuously explored in the last years. Frustration is considered a key ingredient to induce unconventional magnetic orders or even disorder, including spin-liquid states and exotic excitations. In one-dimensional and quasi-one-dimensional models, quantum antiferromagnets show many fascinating magnetic properties at low temperatures which continue to attract an intense theoretical activity. As representative of geometrically frustrated homogeneous spin chains, one can consider the antiferromagnetic spin $S = 1/2$ zig-zag chain (for which compounds such as CuGeO_3 ¹, LiV_2O_5 ² or SrCuO_2 ³ are almost ideal prototypes) and three-leg antiferromagnetic spin tubes (realized in $[(\text{CuCl}_2\text{tachH})_3\text{Cl}]\text{Cl}_2$ ⁴). The chemistry of these compounds enables the synthesis of single crystals much larger than the previously observed organic analogs and, consequently, the achievement of new and more precise experimental studies.

In this context, both experimental and theoretical interest on magnetoelastic chains was triggered by the discovery of the spin-Peierls transition in CuGeO_3 ⁵ at zero magnetization. This transition is an instability due to magnetoelastic effects which is characterized (below a critical temperature T_{SP}) by the opening of a spin gap and the appearance of a dimerized lattice distortion at $M = 0$, with the consequent modulation in spin exchanges. Thus two related issues play together: the lattice distortion represents a cost in elastic energy, while the spin exchange modulation modifies the magnetic spectrum.

A similar phenomenon can be analyzed in magnetoelastic systems at non zero magnetization, appearing as most interesting the systems exhibiting magnetization plateaux. Moreover, it has been shown in Ref. [6] that a spin-phonon interaction in zig-zag chains explains a spin gap opening as well as the presence of non-zero magnetization plateaux at low frustration, where they are indeed absent in the case of non-elastic chains. Such plateaux are due to a mechanism of commensurability between lattice distortions and spin modulation.

Regarding non-elastic zig-zag chains at $M = 1/3$ magnetization plateaux, it was recently shown^{7,8} that small modulations of exchange couplings with period three on top of a homogeneous zig-zag chain can drive a magnetic transition from a three-fold degenerate ground state⁹ to either the so called classical plateau state (CP , where the spin configuration resembles an Ising up-up-down state $\uparrow\uparrow\downarrow$) or the quantum plateau state (QP , where the spin configuration resembles a quantum singlet-up state $\bullet\bullet\uparrow$). Experimental and numerical evidence for a quantum plateau at $M = 1/3$ was recently presented¹⁰ for $\text{Cu}_3(\text{P}_2\text{O}_6\text{OH})_2$, a newly synthesized compound that is very well described by spin $S = 1/2$ antiferromagnetic chains with period three modulated exchange couplings.

Some insight about the magnetoelastic ground state can be obtained from the mentioned fixed modulation results at $M = 1/3$. When one considers a $J_1 - J_2$ chain with only nearest neighbors spin-phonon coupling, a lattice deformation that brings closer two neighbors to the same site (see Fig. 1, upper panel) induces a spin exchange modulation in J_1 forming open trimers. The ground state of the isolated trimer with $S_z = 1/2$ indicates⁷ the pinning of one of the classical plateau states, namely that with $\uparrow\downarrow\uparrow$ order on each trimer. Instead, if two of every three sites group together form-

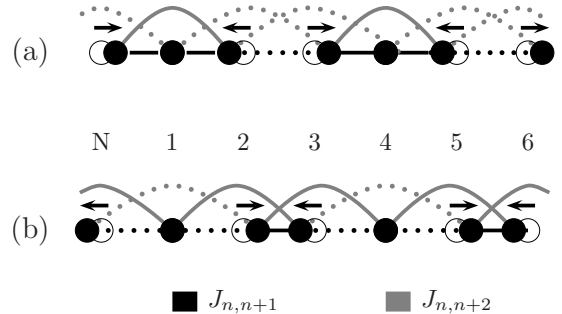


FIG. 1: The upper panel describes a lattice deformation that enhances trimers; the lower panel corresponds to dimer enhancement.

ing dimers (see Fig. 1, lower panel), the chain is driven to the quantum plateau state, that with spin singlets at

each dimer. A different situation arises when one considers also next-nearest neighbors spin-phonon coupling, leading to modulations of both J_1 and J_2 exchanges. The particular modulation discussed in Ref. [8] could be obtained (see again Fig. 1, upper panel) when J_1 and J_2 are modified so as to form closed trimers. In contrast with the previous example, we have shown that in this case trimer enhancement drives this system towards a quantum plateau state. A natural question is then which magnetic configuration corresponds to a given lattice deformation in the general case.

Motivated by the preceding discussion, we investigate in this paper the possibility, suggested by the present authors and collaborators in Ref. [8], of a spin-Peierls like displacive transition in an antiferromagnetic $S = 1/2$ magnetoelastic $J_1 - J_2$ Heisenberg chain, when magnetization is set to $M=1/3$ by an external magnetic field. We explore such a system with both nearest neighbors (NN) and next-nearest neighbors (NNN) spin-phonon couplings in the adiabatic approximation, allowing for modulations of J_1 and J_2 exchanges. This approach follows the recent discussion in Ref. [11], where antiferromagnetic zig-zag spin chain compounds such as $CuGeO_3$ and LiV_2O_5 are argued to present NNN spin-phonon interactions at least of the same order as the NN ones; indeed, a numerical study of such magnetoelastic zig-zag chains at zero magnetization has led to novel tetramerized spin-Peierls like phases.

We show that the magnetoelastic ground state at zero temperature indeed favors several period three distortion patterns, stemming from a competition between elastic energy loss and magnetic energy change. These patterns spontaneously break translation symmetry, with different phases depending on the frustration ratio J_2/J_1 and the value of spin-phonon couplings. As we discuss below, there are essentially four different situations that arise when a lattice deformation of period three generates a spin exchange modulation at $M = 1/3$: the lattice shows two kinds of period three deformation patterns, namely (i) one tending to group three consecutive lattice sites into trimers and (ii) another one tending to group two of every three sites into dimers (see Fig. 1). For each deformation pattern, depending on the microscopic parameters, the spin sector adopts either (a) a classical plateau configuration, pinned in the lattice with the \downarrow spins sitting in the most convenient sites, or (b) a quantum plateau state, with the spin singlets located at some convenient links. A rich phase diagram is built, including all of the combinations of dimer-like and trimer-like deformations with both classical and quantum plateau states.

The paper is organized as follows. In Section II we present the model and its analytical treatment. The spin sector is described within the bosonization approach, while the phonon sector is described in the adiabatic approximation by classical static deformations. In Section III we analyze this effective description by considering all of the relevant perturbation terms as semiclassical po-

tentials, and draw a qualitative phase diagram with our results. Special emphasis is put on the characterization of the ground state phases that result from the combination of frustration and magnetoelastic effects in different parameter ranges. In Section IV we present the results of Lanczos exact diagonalization of small systems, supporting the bosonization results. Finally, in Section V we present a summary and conclusions of the present work.

II. DESCRIPTION OF THE MODEL AND BOSONIZATION APPROACH

We consider the lattice Hamiltonian of a frustrated spin $S = 1/2$ Heisenberg chain, which can be written as

$$H_M = \sum_n \left(J_{n,n+1} \mathbf{S}_n \cdot \mathbf{S}_{n+1} + J_{n,n+2} \mathbf{S}_n \cdot \mathbf{S}_{n+2} \right), \quad (1)$$

where \mathbf{S}_n are spin operators at site n and $J_{n,n+a} > 0$ are antiferromagnetic NN ($a = 1$) and NNN ($a = 2$) spin exchange couplings. An uniform external magnetic field is also coupled to the spins in order to produce a global magnetization $M = 1/3$ ($M = 1$ corresponding to saturation).

The interaction of spins in a homogeneous zig-zag chain ($J_{n,n+1} = J_1$, $J_{n,n+2} = J_2$) with phonons is usually modeled by a linear expansion of the exchange couplings around the non distorted values J_1 and J_2

$$\begin{aligned} J_{n,n+1} &\approx J_1(1 - A(u_{n+1} - u_n)), \\ J_{n,n+2} &\approx J_2(1 - B(u_{n+2} - u_n)), \end{aligned} \quad (2)$$

where u_n is a scalar relevant coordinate for the displacement of ion n from its equilibrium position, and A , B are called the spin-phonon couplings at NN and NNN sites. The total Hamiltonian, including the elastic energy in the adiabatic approximation, is written as

$$\begin{aligned} H_T &= \frac{1}{2} K \sum_n (u_{n+1} - u_n)^2 + \\ &+ \sum_n \left\{ J_1 \mathbf{S}_n \cdot \mathbf{S}_{n+1} + J_2 \mathbf{S}_n \cdot \mathbf{S}_{n+2} \right\} - \\ &- \sum_n \left\{ J_1 A (u_{n+1} - u_n) \mathbf{S}_n \cdot \mathbf{S}_{n+1} + \right. \\ &\left. + J_2 B (u_{n+2} - u_n) \mathbf{S}_n \cdot \mathbf{S}_{n+2} \right\}, \end{aligned} \quad (3)$$

where K is the homogeneous spring stiffness. The first line corresponds to *classical phonons* elastic energy (H_{CP}), the second one to the homogeneous *magnetic* Hamiltonian (H_M) and the rest to the *spin-phonon* interaction (H_I),

$$H_T = H_{CP} + H_M + H_I. \quad (4)$$

Dimensionless parameters, convenient for numerical analysis, are used below. They are introduced using J_1 as

the energy scale as follows: $A \rightarrow \tilde{A} = (J_1/K)^{1/2}A$, $B \rightarrow \tilde{B} = (J_1/K)^{1/2}B$, $u_n \rightarrow \tilde{u}_n = (K/J_1)^{1/2}u_n$ and $J_1, J_2 \rightarrow \alpha = J_2/J_1$.

In order to observe semi-quantitatively the low energy properties of the model given by Eq.(3), we employ the bosonization method which is generally powerful for the description of one-dimensional spin chains (see for instance Ref. [12]).

We start with the homogeneous magnetic Hamiltonian H_M . To obtain the corresponding low-energy theory one first applies the exact Jordan-Wigner transformation mapping spins onto spinless lattice fermions ψ_n , then one introduces a continuum coordinate $x = na$ with a the lattice spacing and writes a linear approximation for the low energy degrees of freedom around the Fermi level in terms of left and right-moving continuum fermions; the Fermi wave-vector k_F depends on the magnetization. For $M = 1/3$ one gets $k_F = \pi/3a$, then

$$\psi_n \approx e^{i\pi n/3}\psi_R(na) + e^{-i\pi n/3}\psi_L(na). \quad (5)$$

The continuum fermions are spinless and massless, allowing for Abelian bosonization; the complete Hamiltonian is finally mapped into a Gaussian term

$$\frac{v}{2} \int dx \left[\frac{1}{K_L} (\partial\phi)^2 + K_L (\partial\tilde{\phi})^2 \right] \quad (6)$$

plus several vertex operators that are kept only when they are commensurate (non-oscillating in space) and constitute relevant perturbations to the Gaussian conformal field theory. Here ϕ is a compactified boson field defined on a circle, $\phi \equiv \phi + \sqrt{\pi}$, and $\tilde{\phi}$ is its dual field defined by $\partial_x \tilde{\phi} = \partial_t \phi$. The parameters v and K_L (Fermi velocity and Tomonaga-Luttinger parameter respectively) depend on the microscopic parameters of the lattice Hamiltonian H_M ; v is proportional to aJ_1 , while K_L is dimensionless.

A particular feature of the $M = 1/3$ situation is that $k_F = \pi/3a$ makes commensurate a triple Umklapp process⁷, providing a perturbation term of the form

$$- \frac{g_3 v}{2\pi^2 a^2} \int dx \cos(3\sqrt{4\pi}\phi) \quad (7)$$

in H_M . The coefficient g_3 is non-universal and, as well as v and K_L , depends on the renormalization group procedure.

It is known numerically^{9,13} that the homogeneous magnetic Hamiltonian H_M describes a gapless Tomonaga-Luttinger (TL) phase for $0 < J_2/J_1 < \alpha_c = 0.56$ ²⁴. For $\alpha_c < J_2/J_1 \lesssim 1.25$ there exists a strong magnetization plateau at $M = 1/3$. Comparison of bosonization with these results shows that the the Tomonaga-Luttinger parameter should be $K_L > 2/9$ for $J_2/J_1 \lesssim \alpha_c$, as this renders the perturbation in Eq. (7) irrelevant. Then the coefficient g_3 flows to zero under the renormalization group and the effective theory describes a gapless TL phase. On the other hand, for $\alpha_c \lesssim J_2/J_1 \lesssim 1.25$, it should be $K_L < 2/9$, making Eq. (7) a relevant perturbation. Thus

this term opens a magnetic gap and explains the magnetization plateau¹⁴ observed in this range. Moreover, the plateau ground state is known to be three-fold degenerate, with translation symmetry spontaneously broken to an up-up-down configuration⁹; such configurations are described by the pinning of the bosonic field in one of the minima of Eq. (7) considered as a semiclassical potential energy¹⁴, provided that $g_3 > 0$. We will in consequence qualitatively represent the plateau by the behavior of the non-universal coefficient $g_3 \geq 0$ as being smooth and non-vanishing only for $\alpha_c \lesssim J_2/J_1 \lesssim 1.25$, with a maximum at some intermediate value of J_2/J_1 . We will not study here the regime $J_2/J_1 > 1.25$, where the $M = 1/3$ plateau is not present; this should be better done by starting with two spin chains with strong exchange J_2 , weakly coupled by a zig-zag interaction J_1 .

Next, we consider the lattice deformations. From the knowledge of the $M = 1/3$ plateau magnetic ground state in the homogeneous $J_1 - J_2$ chain with $J_2/J_1 > \alpha_c$, one can argue that an adiabatic lattice deformation caused by the spin-phonon coupling in Eq. (3) will have period three. This is also supported by bosonization, as such a deformation is commensurate with $k_F = \pi/3a$. Moreover, as discussed in Ref. [6], even for $J_2/J_1 < \alpha_c$ period three deformations cause commensurability of relevant perturbations at $M = 1/3$ and provide a mechanism for a spin gap (magnetization plateau) in this regime. Numerical evidence of the dominance of period three lattice deformations, obtained from self consistent computations, was also given in [6]. A uniform deformation, leading to global size change, can also appear¹¹; this would produce a uniform shift in J_1 and J_2 , which is unessential to our present analysis.

We will consider in this paper the most general period three deformation, without collective displacement, given by

$$u_n = \frac{u_0}{\sqrt{3}} \sin\left(\frac{2\pi}{3}n - \chi\right), \quad (8)$$

with the amplitude u_0 and a relative phase χ as free parameters. Our purpose is to search for the deformation that minimizes the magnetoelastic energy. Once a minimum of the total energy is found, the amplitude u_0 will indicate the deformation strength and the phase χ will relate the deformation pattern to the corresponding spin ground state characterized by the value of ϕ at the potential minimum.

From Eq. (8) the distortion of the NN bond length between sites n and $n + 1$, denoted by $\delta_n = u_{n+1} - u_n$, is parameterized by

$$\delta_n = u_0 \cos\left(\frac{2\pi}{3}\left(n + \frac{1}{2}\right) - \chi\right), \quad (9)$$

while the NNN distortion is given by

$$\delta_{n+1} + \delta_n = u_0 \cos\left(\frac{2\pi}{3}(n+1) - \chi\right). \quad (10)$$

The elastic energy cost associated to deformations in Eq.

(8) reads simply

$$H_{CP}/J_1 = \frac{1}{4}N\tilde{u}_0^2. \quad (11)$$

Finally, we consider the spin-phonon interaction Hamiltonian H_I induced by lattice deformations in Eq. (8). Following the bosonization procedure one generates an extra renormalization of v and K_L and perturbation terms of the form

$$\frac{\tilde{u}_0 v}{2\pi^2 a^2} \int dx \left(f_1 \cos(\sqrt{4\pi}\phi + \chi) + f_2 \cos(2\sqrt{4\pi}\phi - \chi) \right), \quad (12)$$

thus introducing first and second harmonics of the boson field with coefficients proportional to the deformation amplitude \tilde{u}_0 . Notice that these operators are more relevant than the third harmonic in Eq. (7), and should be kept as well in the $J_2/J_1 > \alpha_c$ regime as for $J_2/J_1 < \alpha_c$, as far as $K_L < 1/2$. Even though the coefficients are non-universal and subject to renormalization, it is useful to report that a first order perturbative computation yields $f_1 \sim \tilde{A}(1 - C_1 J_2/J_1)$ and $f_2 \sim -\tilde{A}(1 + C_2 q J_2/J_1)$, where $q = \tilde{B}/\tilde{A}$ and C_1, C_2 are positive constants with $C_2 \ll C_1$. For a qualitative description, we will assume that f_1 and f_2 depend on the microscopic parameters as suggested by these bare expressions.

Putting all together, we can write the complete effective theory as

$$H_T = H_{CP} + H_{free} + V_{eff} \quad (13)$$

where H_{CP} is the classical elastic contribution given in Eq. (11),

$$H_{free} = \frac{v}{2} \int dx \left[\frac{1}{K_L} (\partial\phi)^2 + K_L (\partial\tilde{\phi})^2 \right] \quad (14)$$

is the Gaussian part of the compactified boson action and

$$V_{eff} = \frac{v}{2\pi^2 a^2} \int dx \left[\tilde{u}_0 f_1 \cos(\sqrt{4\pi}\phi + \chi) + \tilde{u}_0 f_2 \cos(2\sqrt{4\pi}\phi - \chi) - g_3 \cos(3\sqrt{4\pi}\phi) \right] \quad (15)$$

is the bosonic self-interaction potential defining a triple sine-Gordon theory¹⁵. Extensive analysis of competition between harmonics in multi-frequency sine-Gordon theories has been performed^{16,17,18}, mainly focused on the double sine-Gordon model. The three-frequency case has also been recently discussed¹⁹. For our purpose it will be enough to perform a semiclassical treatment, as detailed in the next section.

III. SEMICLASSICAL ANALYSIS OF THE EFFECTIVE THEORY

The aim of the present work is to search for the possibility of elastic deformations that lower the magnetoelastic energy with respect to the homogeneous non-deformed case. The simplest analysis of the effective theory obtained in the previous section, which has proved

to be useful in related cases^{7,8,14}, consists in treating the self-interaction terms in Eq. (15) as a classical potential to be evaluated in constant field configurations.

Within this approximation the energy per site depends on three configuration parameters, \tilde{u}_0 , ϕ and χ , and is readily evaluated to

$$\epsilon(\tilde{u}_0, \phi, \chi) \equiv \frac{E}{J_1 N} = \frac{1}{4}\tilde{u}_0^2 - \frac{g_3}{2\pi^2} \cos(3\sqrt{4\pi}\phi) + \frac{\tilde{u}_0}{2\pi^2} (f_1 \cos(\sqrt{4\pi}\phi + \chi) + f_2 \cos(2\sqrt{4\pi}\phi - \chi)), \quad (16)$$

so that the minima can be found analytically. Notice that this expression is invariant under simultaneous shifts $\sqrt{4\pi}\phi \rightarrow \sqrt{4\pi}\phi + 2\pi/3$, $\chi \rightarrow \chi - 2\pi/3$, in relation with the three equivalent locations of period three structures on the chain. This allows to restrict the analysis to $0 < \sqrt{4\pi}\phi \leq 2\pi/3$ without loss of generality. Also a shift $\chi \rightarrow \chi + \pi$ is equivalent to changing the sign of u_0 , allowing to consider $0 \leq \chi < \pi$. We report results within these restricted ranges.

Among several local minima of the potential, the semiclassical energy is always found in one of the following situations:

1. $\sqrt{4\pi}\phi = 2\pi/3$, $\chi = \pi/3$, $\tilde{u}_0 = (f_1 + f_2)/\pi^2$, where the energy is evaluated to

$$\epsilon = -\frac{g_3}{2\pi^2} - \frac{(f_1 + f_2)^2}{4\pi^4}. \quad (17)$$

2. $\sqrt{4\pi}\phi = \pi/3$, $\chi = 2\pi/3$, $\tilde{u}_0 = (f_1 - f_2)/\pi^2$, where the energy is evaluated to

$$\epsilon = \frac{g_3}{2\pi^2} - \frac{(f_1 - f_2)^2}{4\pi^4}. \quad (18)$$

Before drawing a phase diagram, we discuss the physical content of the possible phases. Following the usual bosonization rules to map ϕ to spin variables²⁰, the value $\sqrt{4\pi}\phi = 2\pi/3$ in the first solution indicates that the spin sector adopts a classical plateau configuration CP^7 , which corresponds to selecting one of the $\uparrow\uparrow\downarrow$ degenerate ground states of the homogeneous chain plateau. We will call its energy ϵ_{CP} . The relative phase $\chi = \pi/3$ plays together with the sign of \tilde{u}_0 in determining the elastic deformation. For $f_1 + f_2 > 0$ one finds a trimer-like elastic deformation grouping blocks of three spins (T , see Fig. 1, upper panel); in the opposite case a dimer-like deformation is set, alternating two closer spins with a more separated one (D , see Fig. 1, lower panel). In the second solution, the value $\sqrt{4\pi}\phi = \pi/3$ is not one of the minima of the homogeneous chain potential, but it signals that the spin sector adopts a state that enhances quantum singlets in a $\bullet\bullet\uparrow$ quantum plateau configuration⁷ QP . The corresponding energy will be called ϵ_{QP} . The relative phase $\chi = 2\pi/3$ in this solution indicates that the lattice deformation is dimer-like (D) for $f_1 - f_2 > 0$ and trimer-like (T) otherwise.

Depending on the coefficients f_1 , f_2 and g_3 , which in turn depend on the microscopic parameters, one of these solutions is selected as the global minimum and determines the magnetoelastic ground state phase.

In order to present a schematic phase diagram, we assume the qualitative phenomenological dependence of f_1 , f_2 and g_3 on the microscopic parameters detailed in the previous section. Following Ref. [11] we have chosen a ratio $\tilde{B} = 1.5 \tilde{A}$, which is used in the rest of the paper, as representative of materials where the NNN spin-phonon coupling plays an important role. The magnetoelastic phases found are shown in Fig. 2. We have checked that,

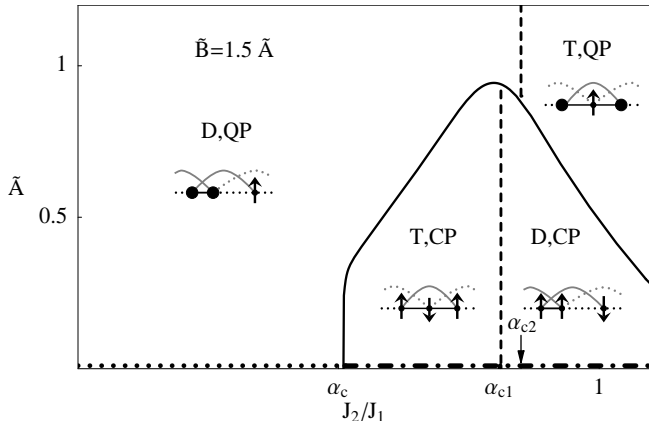


FIG. 2: Schematic magnetoelastic phase diagram with NN and NNN spin-phonon couplings related by $\tilde{B} = 1.5 \tilde{A}$. The classical up-up-down and quantum plateau phases are labelled by CP and QP respectively. The dimer and trimer elastic phases are labelled by D and T . Magnetoelastic patterns in each phase are shown by pictorial diagrams.

within our approximations, all phase transitions result from level crossing of the above described local minima and can be then classified as first order.

For the sake of illustrating the analysis leading to Fig. 2, we show in Fig. 3 the evolution of the energies ϵ_{CP} , ϵ_{QP} as functions of the NN spin-phonon couplings \tilde{A} , $\tilde{B} = 1.5 \tilde{A}$, fixing $J_2/J_1 = 0.7$. This situation lies well inside the homogeneous plateau regime, $J_2/J_1 > \alpha_c$. The coefficients f_1 , f_2 are evaluated according to the first order bare result given in the previous section. The level crossing at $\tilde{A}_c \simeq 0.65$ shows the transition from CP magnetic phase to QP . We remark that this transition is very different than that recently observed by the authors in [8], where the system passes from CP to a Z_2 broken symmetry phase and only then to a QP phase through an Ising like second order transition.

Within each magnetic phase one can also identify the different elastic phases. Given \tilde{A} , we find critical values of J_2/J_1 where \tilde{u}_0 changes sign: in the CP phase, the equation $f_1(\alpha_{c1}) = -f_2(\alpha_{c1})$ defines a critical line $J_2/J_1 = \alpha_{c1}$ such that for $J_2/J_1 < \alpha_{c1}$ the system adopts a trimer like lattice distortion T while for $J_2/J_1 > \alpha_{c1}$ the deformation is dimer like D . In contrast, in the QP phase we find a critical line α_{c2} where $f_1(\alpha_{c2}) = f_2(\alpha_{c2})$,

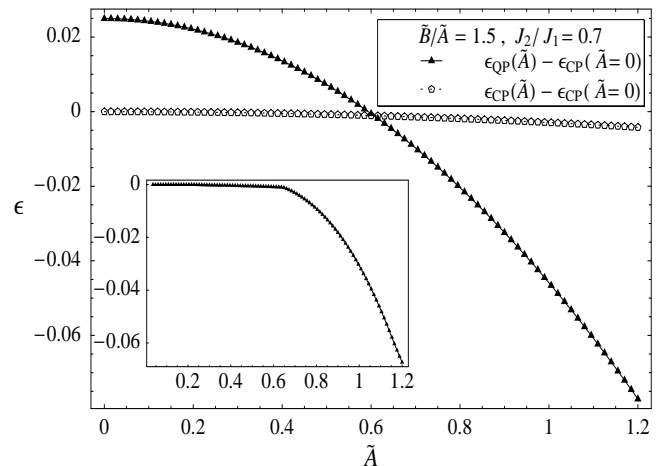


FIG. 3: Semiclassical energies for the classical and quantum plateau minima in terms of the spin-phonon coupling \tilde{A} , for $\tilde{B} = 1.5 \tilde{A}$ and $J_2/J_1 = 0.7$. The inset shows the ground state energy obtained by exact diagonalization of a system with $N = 24$ sites, after fitting the zero-energy level.

being the lattice distortion of type D for $J_2/J_1 < \alpha_{c2}$ and of type T for $J_2/J_1 > \alpha_{c2}$. Using the bare expressions for f_1 , f_2 , these critical lines do not depend on \tilde{A} .

A similar analysis can be made for $J_2/J_1 \lesssim \alpha_c$. The most important difference is that in this region the Tomonaga-Luttinger parameter is $K_L > 2/9$ and the third harmonic is irrelevant. We represent this situation by setting $g_3 = 0$. As mentioned before, the magnetization plateau at $M = 1/3$ is induced by the coupling to the lattice⁶ through the first and second harmonics in Eq. (15). Unlike the previous case, there is no level crossing between ϵ_{QP} and ϵ_{CP} ; the absolute energy minimum always corresponds to ϵ_{QP} , selecting the QP magnetic phase. We also find $(f_1 - f_2) > 0$ in the whole region, so that the elastic phase is of type D .

The relative position of the elastic deformations and the magnetization profile at each phase is determined by the corresponding values of ϕ and χ , as can be found using Eq. (8) and bosonization formulae. The four phases are described by diagrams in Fig. 2.

Different ratios \tilde{B}/\tilde{A} can be analyzed similarly. We have observed that lowering this ratio produces an increase in the region characterized by the classical plateau and trimer-like deformations, with higher values of both α_{c1} and \tilde{A}_c .

It is important to notice that the deformation amplitude \tilde{u}_0 is proportional to f_1 , f_2 , which are in turn proportional to the dimensionless spin-phonon couplings \tilde{A} , \tilde{B} . In Fig. 2, the elastic pattern evolves to the homogeneous limit as $\tilde{A} \rightarrow 0$. By construction, the effective theory in Eqs. (14, 15) describes in this limit a Tomonaga-Luttinger phase for $J_2/J_1 < \alpha_c$ and a gapped sine-Gordon phase with triple degenerate ground state for $J_2/J_1 > \alpha_c$.

It is also interesting to mention that if our approach remains valid in the limit $J_2/J_1 \rightarrow 0$, describing a single NN spin chain, the system adopts a dimer like elastic deformation which in turn induces a trimerized modulation with one larger and two smaller NN spin exchanges (c.f. Fig. 1, lower panel). This model was recently studied by quantum Monte Carlo simulations of large systems in connection with $Cu_3(P_2O_6OH)_2$ ¹⁰, finding exactly the quantum plateau magnetic phase predicted by our analysis.

IV. NUMERICAL ANALYSIS

In order to support the bosonization results in the previous section, we performed a numerical analysis of the Hamiltonian in Eq. (3) by exact diagonalization of small clusters of size up to $N = 24$ sites with periodic boundary conditions.

The strategy is the following: period three elastic deformations without collective displacement are parameterized by two independent bond distortions, say $\delta_1 = u_2 - u_1$ and $\delta_2 = u_3 - u_2$, while $\delta_3 = -\delta_1 - \delta_2$ and $\delta_{n+3} = \delta_n$. For given values of J_2/J_1 and \tilde{A} , fixing \tilde{B}/\tilde{A} and $M = 1/3$, we computed by Lanczos diagonalization²¹ the exact ground state energy of the total Hamiltonian in Eq. (3) for a wide range of elastic deformations ($\delta_1, \delta_2, \delta_3$) and then selected the absolute minimum.

We found that, in accordance with bosonization results, the lowest energy configuration is always obtained (except for equivalent lattice translations) at one of lattice distortions patterns shown in Fig. 1:

1. $(\delta_1, \delta_2, \delta_3) = (-\frac{1}{2}\Delta, -\frac{1}{2}\Delta, \Delta)$ that corresponds to the trimer-like phase (T), or
2. $(\delta_1, \delta_2, \delta_3) = (\frac{1}{2}\Delta, \frac{1}{2}\Delta, -\Delta)$ that corresponds to the dimer-like (D).

In order to characterize the magnetic phases, we also computed the local magnetization profile $\langle S_n^z \rangle$ for the ground state. The order parameter

$$M_S = \frac{1}{N} \sum_n \cos\left(\frac{2\pi}{3}(n-2)\right) \langle S_n^z \rangle \quad (19)$$

introduced in Ref. [8], which is positive for the quantum plateau (QP) configuration and negative for the classical plateau (CP), is used to report the results. We found that both magnetic phases are realized at some region of either the T or the D elastic phases.

A thorough scanning of the $\tilde{A} > 0, J_2/J_1 > 0$ plane was made for $N = 24$ sites, keeping $\tilde{B} = 1.5\tilde{A}$. The magnetoelastic phases found are shown in Fig. 4. Representative scans at $J_2/J_1 = 0.3, 0.6, 0.9$ are shown in Fig. 5, showing $\delta_1, \delta_2, \delta_3$ and M_S as functions of \tilde{A} . Notice that the deformation amplitude decreases for small \tilde{A} (a limit that corresponds to large stiffness K); due to finite size effects²² there is no deformation below

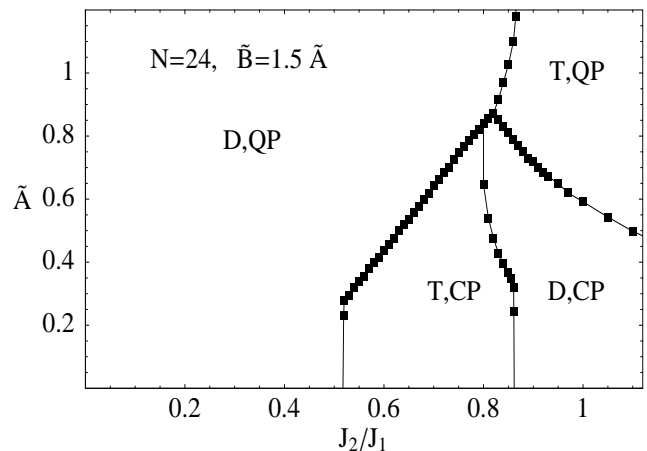


FIG. 4: Magnetoelastic phase diagram obtained by exact diagonalization of $N = 24$ sites. Spin-phonon couplings ratio is set to $\tilde{B}/\tilde{A} = 1.5$.

some finite value of \tilde{A} , which is seen to diminish with size by comparing $N = 12, 18, 24$ sites. The $J_2/J_1 = 0.3$ scan shows the phase D, QP for all \tilde{A} . In the $J_2/J_1 = 0.6$ case one can clearly observe the first order transition at some value of \tilde{A} (which in general depends on J_2/J_1), with finite jumps both in the deformations and the magnetic order parameter, from the T, CP to the D, QP phase. The same happens in the $J_2/J_1 = 0.9$ case, with a transition from the D, CP to the T, QP phase. The region $0.8 < J_2/J_1 < 0.9$ shows that the critical line for transition between T and D phases slightly depends on J_2/J_1 ; comparison with Fig. 2 indicates that renormalization effects on the bare coefficients f_1, f_2 are not strong enough to impede our qualitative bosonization analysis.

We have also analyzed different spin-phonon couplings, confirming the bosonization prediction that lowering the ratio \tilde{B}/\tilde{A} produces an increase in the region characterized by the classical plateau and trimer-like deformations (c.f. Fig. 2), with higher values of both α_{c1} and \tilde{A}_c .

In summary, the numerical results confirm the semiclassical analysis given in previous section.

V. CONCLUSIONS

In the present work we have shown the existence of different magnetoelastic phases in $S = 1/2$ zig-zag antiferromagnetic $J_1 - J_2$ chains coupled to adiabatic phonons through nearest and next-nearest neighbor spin exchanges, at $M = 1/3$ magnetization. At zero temperature this situation corresponds to a magnetization plateau, either existing for the non-distorted homogeneous chain with high enough frustration^{9,14} or induced by spin-phonon coupling at lower frustration⁶.

We performed a semiclassical analysis of the bosonized effective theory, supported by numerical exact diagonalization of small clusters up to 24 spins. We found that several spin-Peierls like phases describe the ground state

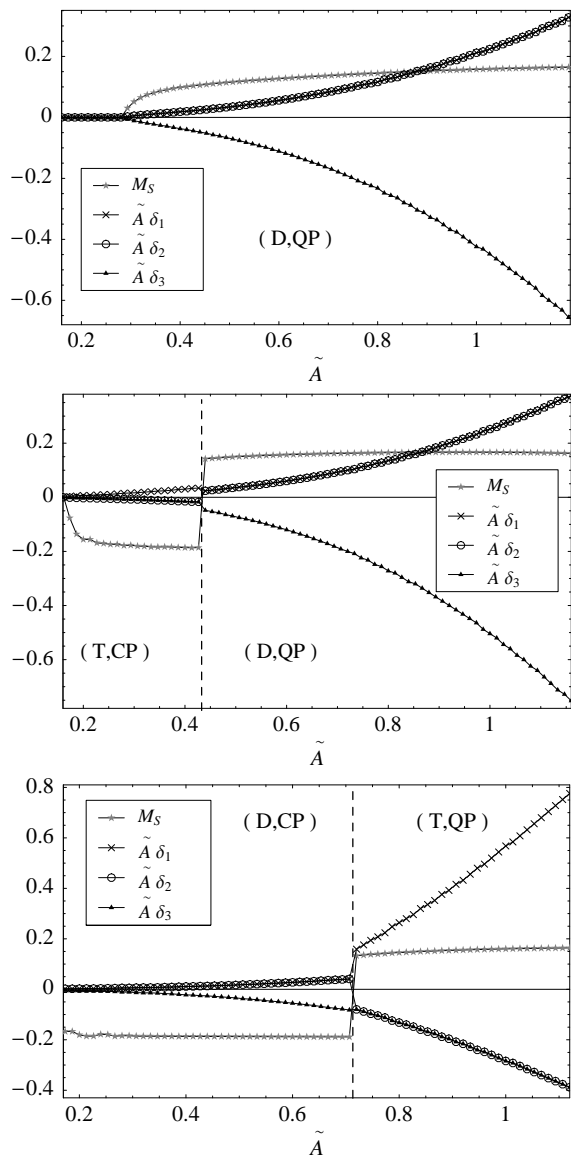


FIG. 5: Lattice distortions $\delta_{1,2,3}$ and order parameter M_S as a function of \tilde{A} for $\tilde{B}/\tilde{A} = 1.5$ and $J_2/J_1 = 0.3$ (upper panel), 0.6 (middle panel), 0.9 (lower panel). Each panel corresponds to a vertical scan in Fig. 4. Small \tilde{A} is not accessible due to finite size effects.

of the system, depending on the microscopic parameters J_2/J_1 and spin-phonon couplings. In each of these phases a non trivial elastic deformation is favored, grouping together blocks of two or three spins, while the magnetic sector adopts classical or quantum plateau states.

A detailed analysis of a particular case, chosen as representative of materials with large ratio of next-nearest to nearest neighbors spin-phonon couplings¹¹, shows the following magnetoelastic phases at zero temperature:

- (i) an up-up-down magnetic phase with a trimer-like lattice distortion when frustration is just enough to produce the $M = 1/3$ magnetization plateau in the homogeneous chain and spin-phonon couplings are low.
- (ii) an up-up-down magnetic phase with a dimer-like lattice distortion for low spin-phonon couplings and higher frustration.
- (iii) a quantum plateau magnetic phase with dimer-like lattice distortion for large spin-phonon couplings and low frustration. This phase is present even for such low frustrations that would not produce a magnetization plateau in absence of spin-phonon interaction.
- (iv) a quantum plateau magnetic phase with trimer-like lattice distortion for large spin-phonon couplings and high frustration.

Once the existence of non trivial magnetoelastic phases at zero temperature is proved, a natural question is to analyze the possibility of a spin-Peierls like transition in three dimensional materials with quasi-one-dimensional magnetic structure. Since a high temperature phase is expected to recover translation invariance, such a transition could take place at some finite temperature²³, while an external magnetic field maintains the magnetization $M = 1/3$. However, a finite temperature study should also take into account the eventual smoothing of the magnetization plateau. The critical temperature and the behavior of thermodynamic functions at the conjectured transition is suggested for future investigation.

Acknowledgments: the authors thank T. Vekua for bringing attention into the subject, A.O. Dobry and D.C. Cabra for valuable comments and M.D. Grynberg for numerical assistance in Lanczos diagonalization. This work was partially supported by CONICET (Argentina), PICT ANCYPT (Grant 20350), and PIP CONICET (Grant 5037).

¹ For a review, see *e.g.* J.-P. Boucher and L.-P. Regnault, J. Phys. I (France) **6**, 1939 (1996).
² M. Isobe and Y. Ueda, J. Phys. Soc. Jpn. **65**, 3142 (1996); N. Fujiwara, H. Yasuoka, M. Isobe, Y. Ueda, and S. Maegawa, Phys. Rev. B **55**, R11945 (1997).
³ M. Matsuda and K. Katsumata, J. Magn. Magn. Mater. **140**, 1671 (1995).
⁴ J. Schnack, H. Nojiri, P. Kögerler, G.J.T. Cooper, and L. Cronin, Phys. Rev. B **70**, 174420 (2004); J.-B. Fouet, A. Lauchli, S. Pilgram, R.M. Noack, and F. Mila, Phys. Rev.

B **73**, 014409 (2006).

⁵ M. Hase, I. Terasaki, and K. Uchinokura, Phys. Rev. Lett. **70**, 3651 (1993).

⁶ T. Vekua, D.C. Cabra, A.O. Dobry, C.J. Gazza, and D. Poilblanc, Phys. Rev. Lett. **96**, 117205 (2006); C.J. Gazza, A.O. Dobry, D.C. Cabra, and T. Vekua, Phys. Rev. B **75**, 165104 (2007).

⁷ K. Hida and I. Affleck, J. Phys. Soc. Jpn. **74**, 1849 (2005).

⁸ H.D. Rosales, D.C. Cabra, M.D. Grynberg, G.L. Rossini, and T. Vekua, Phys. Rev. B **75**, 174446 (2007).

- ⁹ K. Okunishi and T. Tonegawa, J. Phys. Soc. Jpn. **72**, 479 (2003).
- ¹⁰ M. Hase, M. Kohno, H. Kitazawa, N. Tsujii, O. Suzuki, K. Ozawa, G. Kido, M. Imai, and X. Hu, Phys. Rev. B **73**, 104419 (2006).
- ¹¹ F. Becca, F. Mila, and D. Poilblanc, Phys. Rev. Lett. **91**, 067202 (2003).
- ¹² T. Giamarchi, *Quantum Physics in One Dimension* (Oxford University Press, Oxford, 2004).
- ¹³ T. Tonegawa, K. Okamoto, K. Okunishi, K. Nomura, and M. Kaburagi, Physica B **346-347**, 50 (2004).
- ¹⁴ P. Lecheminant and E. Orignac, Phys. Rev. B **69**, 174409 (2004).
- ¹⁵ M. Høgh Jensen and P.S. Lomdahl, Phys. Rev. B **26**, 1086 (1982).
- ¹⁶ G. Delfino and G. Mussardo, Nucl. Phys. B **516**, 675 (1998).
- ¹⁷ M. Fabrizio, A.O. Gogolin, and A.A. Nersisyan, Nucl. Phys. B **580**, 647 (2000).
- ¹⁸ Z. Bajnok, L. Palla, G. Takacs, and F. Wagner, Nucl. Phys. B **601**, 503 (2001).
- ¹⁹ G.Z. Tóth, J. Phys. A **37**, 9631 (2004).
- ²⁰ See for instance D.C. Cabra and P. Pujol, in *Quantum Magnetism*, Lect. Notes Phys. **645** (2004).
- ²¹ See for example, G. H. Golub and C. F. van Loan, *Matrix Computations*, 3rd. ed. (Johns Hopkins University Press, Baltimore, 1996).
- ²² A.E. Feiguin, J.A. Riera, A. Dobry, and H.A. Ceccatto, Phys. Rev. B **56**, 14607 (1997).
- ²³ See for instance A. Dobry, D.C. Cabra, and G.L. Rossini, Phys. Rev. B **75**, 045122 (2007), and references therein.
- ²⁴ The critical value for J_2/J_1 has also been reported as 0.487 using level spectroscopy, see Ref. [13].